*Inorg. Chem.* **2005**, *44*, 4301–4308


# Steric Effects in Metathesis and Reduction Reactions of Phosphinimines with Catechol- and Pinacolboranes

**Sarah Hawkeswood, Pingrong Wei, James W. Gauld, and Douglas W. Stephan***

*Department of Chemistry & Biochemistry, University of Windsor, Windsor, Ontario, Canada N9B 3P4*

Received February 14, 2005

A series of catecholboryl–phosphinimide complexes with the general formula $(\mu\text{-}(R_3PN)Bcat)_x$ (cat = $O_2C_6H_4$) have been synthesized via associative metathetical reactions. For R = Et, *n*-Bu, Ph, and *i*-Pr and $R_3$ = *n*-Bu *t*-$Bu_2$ X-ray crystallography as well as solution NMR spectroscopy and reactivity studies reveal that these species are dimeric. In the case of R = *t*-Bu, the steric congestion results in the monomeric species, *t*-$Bu_3$PNBcat. Similarly, reactions of R(*t*-$Bu)_2$PNH (R = *n*-Bu, *t*-Bu) and *i*-$Pr_3$PNH with pinacolborane ($HBO_2C_2Me_4$ = HBpin) led to the formation of *n*-Bu(*t*-$Bu_2$)PNBpin, *t*-$Bu_3$PNBpin, and *i*-$Pr_3$PNBpin. Analogous reactions of smaller phosphinimines $R_3$PNH (R = Et or *n*-Bu) with pinacolborane (HBpin) generated free phosphine and the boron-containing product HN$(Bpin)_2$. In the related reactions of $R_3$PNPh or $R_3$PNAd (R = Et and *n*-Bu) and HBpin, the white crystalline solids PhHN(Bpin) or AdHN(Bpin) were isolated. HN$(Bpin)_2$ was also derived from the reaction of $Et_3PNSiMe_3$ and HBpin. Kinetic studies showed this reaction is first order in both reagents with a rate constant of $1.3(7) \times 10^{-4}$ $s^{-1}$. A mechanism involving a 1:1 donor–acceptor interaction of the phosphinimine and borane affording reduction of the phosphinimine to phosphine with concurrent formation of borylamine is proposed. Computational studies were performed to probe the steric effects on these reactions of phosphinimine and borane. Model reactions involving *t*-$Bu_3$PNH showed a lower activation barrier for protonolysis in comparison to phosphinimine reduction. In contrast, for the smaller phosphinimine $H_3$PNH, the activation barriers for phosphinimine reduction are lower. The causes of these steric effects are considered.

## Introduction

Phosphinimine and phosphinimide complexes of main group elements and transition metals have been shown to exhibit wide structural diversity.[1,2] Recently, reactivity studies of such compounds have drawn considerable attention. We have shown that early transition metal derivatives can yield highly effective catalysts for olefin polymerization.[3−7] Meyer and co-workers have demonstrated that phosphinimines themselves undergo metathesis with imines and catalyze imine/imine and imine/carbodiimine cross-metathesis.[8,9] Moreover, phosphinimine-based ligands have been employed to support novel transition metal complexes,[10−13] while theoretical studies have examined the electronic nature of phosphinimines and phosphinimide complexes.[14−16] Understand-

* Author to whom correspondence should be sent. E-mail: stephan@uwindsor.ca.

(1) Dehnicke, K.; Krieger, M.; Massa, W. *Coord. Chem. Rev.* **1999**, *182*, 19−65.
(2) Dehnicke, K.; Weller, F. *Coord. Chem. Rev.* **1997**, *158*, 103−169.
(3) Hollink, E.; Wei, P.; Stephan, D. W. *Organometallics* **2004**, *23*, 1562−1569.
(4) Stephan, D. W.; Guerin, F.; Spence, R. E. v. H.; Koch, L.; Gao, X.; Brown, S. J.; Swabey, J. W.; Wang, Q.; Xu, W.; Zoricak, P.; Harrison, D. G. *Organometallics* **1999**, *18*, 2046−2048.
(5) Stephan, D. W.; Stewart, J. C.; Guerin, F.; Courtenay, S.; Kickham, J.; Hollink, E.; Beddie, C.; Hoskin, A.; Graham, T.; Wei, P.; Spence, R. E. v. H.; Xu, W.; Koch, L.; Gao, X.; Harrison, D. G. *Organometallics* **2003**, *22*, 1937−1947.
(6) Stephan, D. W.; Stewart, J. C.; Guerin, F.; Spence, R. E. v. H.; Xu, W.; Harrison, D. G. *Organometallics* **1999**, *18*, 1116−1118.
(7) Yue, N.; Hollink, E.; Guerin, F.; Stephan, D. W. *Organometallics* **2001**, *20*, 4424−4433.
(8) Bell, S. A.; Meyer, T. Y.; Geib, S. J. *J. Am. Chem. Soc.* **2002**, *124*, 10698−10705.
(9) Burland, M. C.; Meyer, T. Y. *Inorg. Chem.* **2003**, *42*, 3438−3444.
(10) Aparna, K.; Babu, R. P. K.; McDonald, R.; Cavell, R. G. *Angew. Chem., Int. Ed.* **2001**, *40*, 4400−4402.
(11) Babu, R. P. K.; McDonald, R.; Cavell, R. G. *Chem. Commun.* **2000**, *006*, 481−482.
(12) Kasani, A.; Babu, R. P. K.; McDonald, R.; Cavell, R. G. *Angew. Chem., Int. Ed.* **1999**, *38*, 1483−1484.
(13) Kasani, A.; McDonald, R.; Cavell, R. G. *Chem. Commun.* **1999**, 1993−1994.
(14) Sundermann, A.; Uzan, O.; Milstein, D.; Martin, J. M. L. *J. Am. Chem. Soc.* **2000**, *122*, 7095−7104.
(15) Lu, W. C.; Sun, C. C. *THEOCHEM* **2002**, *593*, 1−7.
(16) Xue, Y.; Kim, C. K. *J. Phys. Chem. A* **2003**, *107*, 7945−7951.

10.1021/ic050230k CCC: $30.25 
Published on Web 05/17/2005

ing the structure−reactivity relationship continues to stimulate research endeavors. In our work to uncover strategies to improved olefin polymerization catalysts, one recurring theme has emerged: the resulting reactivity of phosphinimide complexes is determined by the admixture of the polarity of the P−N bond and the steric demands of the substituents on phosphorus.[17−19] In an effort to probe the generality of these observations, we have begun to examine related main group−phosphinimide chemistry. Initially we probed the role of the steric demands and showed that while phosphinimines with small substituents were known to afford species of formula $B(NPR_3)_3$,[20] sterically demanding phosphinimines gave the linear borinium salt $[(t\text{-}Bu_3PN)_2B]Cl$.[21] Similar steric effects were observed in methyl-abstraction reactions of silyl and tin phosphinimines.[22] Herein we describe steric effects on the reactions of phosphinimines with catechol and pinacolboranes.

## Experimental Section

**General Data.** All preparations were performed under an atmosphere of dry $O_2$-free $N_2$ by employing either Schlenk-line techniques or a Vacuum Atmospheres glovebox. Solvents were purified employing Grubbs-type column systems manufactured by Innovative Technologies or were distilled from the appropriate drying agents under $N_2$. ClBcat, HBpin, *n*-$Bu_3P$, $Et_3P$, and $N_3SiMe_3$ were used as received from Sigma-Aldrich. *t*-$Bu_3P$ and *i*-$Pr_3P$ were purchased from the Strem Chemical Co. Modified literature procedures were used to synthesize the phosphinimines.[5] $^1H$, $^{13}C\{^1H\}$, $^{31}P\{^1H\}$, $^{11}B\{^1H\}$, and $^{19}F\{^1H\}$ NMR spectra were recorded on Bruker Avance spectrometers operating at 300 and 500 MHz, respectively. Deuterated benzene and toluene were purchased from Cambridge Isotopes Laboratories, vacuum distilled from the appropriate drying agents, and freeze−pump−thaw-degassed (3×). $C_6D_6$ was used to record the NMR spectra unless otherwise indicated. Trace amounts of protonated solvents were used as references, and $^1H$ and $^{13}C\{^1H\}$ NMR chemical shifts ($\delta$) are reported relative to $SiMe_4$. $^{31}P\{^1H\}$, $^{11}B\{^1H\}$, and $^{19}F\{^1H\}$ NMR spectra are referenced to 85% $H_3PO_4$, $BF_3(OEt_2)$ and $CFCl_3$, respectively. Line widths at half-height ($\Delta\nu_{1/2}$) are reported in hertz. Combustion analyses were performed at the University of Windsor Chemical Laboratories. Infrared spectra were collected on a Bruker Vector 22 FT-IR spectrometer using Nujol mulls. Modified literature procedures were used to synthesize *t*-$Bu_3PNSiMe_3$, *i*-$Pr_3PNSiMe_3$, *n*-$Bu_3PNPh$, $Et_3PNAd$, $Et_3PNH$, *n*-$Bu_3PNH$, *t*-$Bu_3PNH$, $PhN_3$, $Et_3PNH$, and *n*-$Bu_3PNH$.[23−29]

**Synthesis of $((\mu\text{-}R_3PN)Bcat)_2$ ($R_3$ = $Et_3$ (1), *n*-$Bu_3$ (2), $Ph_3$ (3), *i*-$Pr_3$ (4), *n*-But-$Bu_2$ (5)), and *t*-$Bu_3$PNBcat (6).** These compounds were prepared in a similar fashion, and thus, only one preparation is detailed. A solution of ClBcat (0.270 g, 1.75 mmol) in 20 mL of toluene was added to a solution of $Et_3PNSiMe_3$ (0.360 g, 1.75 mmol) in 2 mL of toluene and was stirred for 1 h at room temperature. Toluene and $SiMe_3Cl$ were removed in vacuo. The product was washed with pentanes (3 × 2 mL) and dried in vacuo. A white solid was isolated. Data for **1**: yield 82%; $^1H$ NMR 7.10 (m, 4H, $C_6H_4$ (*o*-H)), 6.89 (m, 4H, $C_6H_4$ (*m*-H)), 1.22 (dq, 12H, $CH_2$, $^2J_{P-H}$ = 12 Hz, $^3J_{H-H}$ = 8 Hz), 0.73 (dt, 18H, Me, $^3J_{P-H}$ = 17 Hz, $^3J_{H-H}$ = 8 Hz); $^{31}P\{^1H\}$ NMR 40.7; $^{13}C\{^1H\}$ NMR 153.4 (s, $C_6H_4$ (*ipso*-C)), 119.0 (s, $C_6H_4$ (*o*-C)), 109.2 (s, $C_6H_4$ (*m*-C)), 16.9, 5.7 (s, Me); $^{11}B\{^1H\}$ NMR 8.1. Anal. Calcd: H, 7.63; C, 57.41; N, 5.58. Found: H, 7.67; C, 57.59; N, 5.55. Data for **2**: yield 97%; $^1H$ NMR ($C_6D_6$) 7.02 (m, 4H, $C_6H_4$ (*o*-H)), 6.84 (m, 4H, $C_6H_4$ (*m*-H)), 1.36 (m, 24H, $CH_2CH_2$), 1.07 (m, 12H, $PCH_2$), 0.76 (t, 18H, Me, $^3J_{H-H}$ = 7.2 Hz); $^{31}P\{^1H\}$ NMR 35.9; $^{13}C\{^1H\}$ NMR 153.4 (s, $C_6H_4$ (*ipso*-C)), 118.9 (s, $C_6H_4$ (*o*-C)), 109.2 (s, $C_6H_4$ (*m*-C)), 25.7 (s, $PCH_2$), 24.8 (s, $PCH_2CH_2$), 24.0 (s, $PCH_2CH_2$), 14.0 (s, Me); $^{11}B\{^1H\}$ NMR 6.0. Anal. Calcd: H, 9.32; C, 64.49; N, 4.18. Found: H, 9.77; C, 64.25; N, 4.09. Data for **3**: yield 69%; $^1H$ NMR ($C_6D_5CD_3$ ) 7.70 (dd, 12H, PPh, $^3J_{P-H}$ =13 Hz, $^3J_{H-H}$ = 8 Hz), 6.99 (m, 22H, PPh, $C_6H_4$), 6.75 (m, 4H, $C_6H_4$); $^{31}P\{^1H\}$ NMR ($C_6D_5CD_3$) 34.1; $^{13}C\{^1H\}$ NMR ($C_6D_5CD_3$, partial) 132.8 (PPh), 131.8 (PPh), 128.8 (PPh), 121.3 ($C_6H_4$), 111.5 ($C_6H_4$); $^{11}B\{^1H\}$ NMR ($C_6D_5CD_3$) 8.4. Anal. Calcd: H, 4.85; C, 72.94; N, 3.54. Found: H, 5.07; C, 72.61; N, 3.58. Data for **4**: yield 83%; $^1H$ NMR ($C_6D_5CD_3$) 6.95 (m, 4H, $C_6H_4$ (*o*-H)), 6.76 (m, 4H, $C_6H_4$ (*m*-H)), 1.82 (dseptet, 6H, *i*-Pr, $^2J_{P-H}$ = 12 Hz, $^3J_{H-H}$ = 7 Hz), 0.96 (dd, 36H, *i*-Pr, $^3J_{P-H}$ = 15 Hz, $^3J_{H-H}$ = 7 Hz); $^{31}P\{^1H\}$ NMR ($C_6D_5CD_3$) 49.2; $^{13}C\{^1H\}$ NMR ($C_6D_5CD_3$) 153.0 ($C_6H_4$ (*o*-C)), 121.6 ($C_6H_4$ (*o*-C)), 109.1 ($C_6H_4$ (*m*-C)), 25.2 (d, *i*-Pr), 17.2 (*i*-Pr); $^{11}B\{^1H\}$ NMR ($C_6D_5CD_3$) 7.8. Anal. Calcd: H, 8.60; C, 61.46; N, 4.78. Found: H, 8.48; C, 61.23; N, 4.65. Data for **5**: yield 60%; $^1H$ NMR 7.09 (m, 4H, $C_6H_4$ (*o*-H)), 6.80 (m, 4H, $C_6H_4$ (*m*-H)), 1.67 (m, 4H, $PCH_2$), 1.49 (m, 4H, $CH_2CH_2$), 1.26 (m, 4H, $CH_2Me$), 1.03 (d, 36H, *t*-Bu, $^3J_{P-H}$ = 14 Hz), 0.83 (t, 6H, Me, $^3J_{H-H}$ = 7 Hz); $^{31}P\{^1H\}$ NMR 38.8; $^{13}C\{^1H\}$ NMR 151.1 (s, $C_6H_4$ (*ipso*-C)), 121.4 (s, $C_6H_4$ (*o*-C)), 111.5 (s, $C_6H_4$ (*m*-C)), 36.6 (d, *t*-Bu, $^1J_{P-C}$ = 62 Hz), 27.4 (s, *t*-Bu, 26.5 (d, $CH_2$, $^3J_{P-C}$ = 13 Hz), 25.4 (d, $CH_2CH_2$, $^3J_{P-C}$ = 13 Hz), 22.18 (d, $CH_2Me$, $^3J_{P-C}$ = 57 Hz), 14.7 (s, Me); $^{11}B\{^1H\}$ NMR 24.4. Anal. Calcd: H, 9.32; C, 64.49; N, 4.18. Found: H, 9.29; C, 64.71; N, 4.18. Data for **6**: yield 94%; $^1H$ NMR ($C_6D_5CD_3$) 7.09 (m, 2H, $C_6H_4$ (*o*-H)), 6.81 (m, 2H, $C_6H_4$ (*m*-H)), 1.19 (d, 27H, *t*-Bu, $^3J_{P-H}$ = 13 Hz); $^{31}P\{^1H\}$ NMR ($C_6D_5CD_3$) 42.7; $^{13}C\{^1H\}$ NMR 151.2 (s, $C_6H_4$ (*ipso*-C)), 121.2 (d, $C_6H_4$ , $J$ = 25 Hz), 111.4 (d, $C_6H_4$, $J$ = 28 Hz), 40.4 (d, *t*-Bu, $^1J_{P-C}$ = 53 Hz), 29.7 (s, *t*-Bu); $^{11}B\{^1H\}$ NMR ($C_6D_5CD_3$) 24.2. Anal. Calcd: H, 9.32; C, 64.49; N, 4.18. Found: H, 9.44; C, 64.10; N, 4.29.

**Synthesis of $(\mu\text{-}Et_3PN)Bcat(B(C_6F_5)_3)$ (7).** X (0.034 g, 0.135 mmol) was dissolved in 3 mL of toluene. To this solution was added solid $B(C_6F_5)_3$ (0.069 g, 0.135 mmol). The resulting solution was stirred at ambient temperature for 10 min. The solvent was removed in vacuo, and the resulting white solid was isolated in 82% yield: $^1H$ NMR 6.78 (m, 2H, $C_6H_4$ (*o*-H)), 6.64 (m, 2H, $C_6H_4$ (*m*-H)), 1.65 (dq, 6H, $PCH_2$, $^2J_{P-H}$ = 13 Hz, $^3J_{H-H}$ = 8 Hz), 0.38 (dt, 9H, Me, $^3J_{P-H}$ = 19 Hz, $^3J_{H-H}$ = 8 Hz); $^{31}P\{^1H\}$ NMR 68.0; $^{13}C\{^1H\}$ NMR ($C_6D_5CD_3$) 147.0 (s, $BC_6F_5$), 140.0 (s, $C_6H_4$ (*ipso*-C)), 139.1 (s, $BC_6F_5$), 135.3 (s, $BC_6F_5$), 122.7 (s, $C_6H_4$ (*o*-C)), 111.7 (s, $C_6H_4$ (*m*-C)), 17.6 (d, $PCH_2$, $^1J_{P-C}$ = 60 Hz), 5.9 (s, Me); $^{11}B\{^1H\}$ NMR 28.0 (BO), −6.4; $^{19}F\{^1H\}$ NMR −162.4, −156.4, −131.8. Anal.


(17) Kickham, J. E.; Guerin, F.; Stephan, D. W. *J. Am. Chem. Soc.* **2002**, *124*, 11486−11494.
(18) Kickham, J. E.; Guerin, F.; Stewart, J. C.; Stephan, D. W. *Angew. Chem., Int. Ed.* **2000**, *39*, 3263−3266.
(19) Kickham, J. E.; Guerin, F.; Stewart, J. C.; Urbanska, E.; Ong, C. M.; Stephan, D. W. *Organometallics* **2001**, *20*, 1175−1182.
(20) Moehlen, M.; Neumueller, B.; Dehnicke, K. *Z. Anorg. Allg. Chem.* **1998**, *624*, 177−178.
(21) Courtenay, S.; Mutus, J. Y.; Schurko, R. W.; Stephan, D. W. *Angew. Chem., Int. Ed.* **2002**, *41*, 498−501.
(22) Courtenay, S.; Ong, C. M.; Stephan, D. W. *Organometallics* **2003**, *22*, 818−825.
(23) Aksnes, G.; Froeyen, P. *Acta Chem. Scand.* **1969**, *23*, 2697−703.
(24) Birkofer, L.; Kim, S. M. *Chem. Ber.* **1964**, *97*, 2100−1.
(25) Froeyen, P. *Acta Chem. Scand.* **1972**, *26*, 1777−82.
(26) Lindsay, R. O.; Allen, C. F. H. *Org. Synth.* **1942**, *22*, 96−8.
(27) Staudinger, H.; Meyer, J. *Helv. Chim. Acta* **1919**, *2*, 635−46.
(28) Wiegraebe, W.; Bock, H. *Chem. Ber.* **1968**, *101*, 1414−27.
(29) Wolfsberger, W. *Z. Naturforsch., B* **1978**, *33B*, 1452−6.

Calcd: H, 2.58; C, 48.60; N, 1.89. Found: H, 2.37; C, 48.55; N, 1.79.

**Synthesis of *n*-Bu(*t*-Bu$_2$)PNBpin (8), *t*-Bu$_3$PNBpin (9), and *i*-Pr$_3$PNBpin (10).** These compounds were prepared in a similar fashion, and thus only one preparation is detailed. To a solution of *n*-Bu(*t*-Bu)$_2$PNH (0.050 g, 0.23 mmol) in 3 mL of pentane was added HBpin (0.067 mL, 0.46 mmol). Gas evolution was observed upon addition of HBpin. The resulting solution was stirred at room temperature for 8 h. The solvent and excess HBpin were decanted, and the solid was dried in vacuo and collected. Data for **8**: yield 61%; $^1$H NMR 1.72 (m, 2H, $PCH_2$), 1.50 (m, 2H, $PCH_2CH_2$), 1.30 (sextet, 2H, $CH_2CH_2Me$, $^3J_{H-H}$ = 7 Hz), 1.19 (s, 12H, OCMe), 1.11 (d, 18H, *t*-Bu, $^3J_{P-H}$ = 13 Hz), 0.89 (t, 3H, $CH_2Me$, $^3J_{H-H}$ = 7 Hz); $^{31}$P{$^1$H} NMR 36.2; $^{13}$C{$^1$H} NMR 80.1 (s, OCMe), 36.7 (d, *t*-Bu, $^1J_{P-C}$ = 61 Hz), 27.7 (s, *t*-Bu), 26.6 (d, $CH_2CH_2CH_2$, $^3J_{P-C}$ = 26 Hz), 25.6 (d, $PCH_2CH_2$), 25.1 (s, OCMe), 22.5 (d, $PCH_2$, $^1J_{P-C}$ = 56 Hz), 14.4 (s, $CH_2Me$); $^{11}$B{$^1$H} NMR 22.6. Anal. Calcd: H, 11.45; C, 62.98; N, 4.08. Found: H, 9.80; C, 61.97; N, 3.64. Data for **9**: yield 94%; $^1$H NMR 1.27 (d, 27H, *t*-Bu, $^3J_{P-H}$ = 13 Hz), 1.24 (s, 12H, Me); $^{31}$P{$^1$H} NMR 40.2; $^{13}$C{$^1$H} NMR 80.1 (s, BOC), 40.5 (d, *t*-Bu, $^1J_{P-C}$ = 26 Hz), 30.0 (s, *t*-Bu), 25.6 (s, Me); $^{11}$B{$^1$H} NMR 23.4 ($\Delta\nu_{1/2}$ = 486 Hz). Anal. Calcd: C, 62.98; H, 11.45; N, 4.08. Found: C, 62.85; H, 11.43; N, 4.07. Data for **10**: yield 87%; $^1$H NMR 1.86 (d septet, 3H, $CHMe_2$, $^3J_{P-H}$ = 11 Hz, $^3J_{H-H}$ = 7 Hz), 1.22 (s, 12H, CMe), 1.03 (dd, 18H, $CHMe_2$, $^3J_{P-H}$ = 15 Hz, $^3J_{H-H}$ = 7 Hz); $^{31}$P{$^1$H} NMR 36.0; $^{13}$C{$^1$H} NMR 80.1 (CMe), 25.7 (d, *i*-Pr, $^1J_{P-C}$ = 61 Hz), 25.5 (CMe), 17.5 (*i*-Pr); $^{11}$B{$^1$H} NMR 23.9. Anal. Calcd: H, 11.04; C, 59.81; N, 4.65. Found: H, 11.52; C, 57.61; N, 5.50.

**Synthesis of HN(Bpin)$_2$ (11). Method i.** HBpin (0.10 mL, 0.68 mmol) was slowly added to a pentane solution of *n*-Bu$_3$PNH (0.074 g, 0.34 mmol). Immediate gas evolution was observed. The solution was stirred at 25 °C for 2 h and concentrated to 1 mL from which a white precipitate was collected. The solid was dried in vacuo. This solid was redissolved in pentane from which X-ray-quality crystals of HN(Bpin)$_2$ were grown in 25% yield.

**Method ii.** HBpin (0.81 mL, 5.60 mmol) was slowly added to a pentane solution of Et$_3$PNH (0.355 g, 2.67 mmol). Immediate gas evolution was observed. The solution was stirred at 25 °C for 2 h. The solvent, Et$_3$P, and excess HBpin were removed in vacuo. The resulting white solid was washed (3 × 1 mL) with cold pentane, dried in vacuo, and isolated: yield 92%; $^1$H NMR (partial) 1.04 (s, 24H, Me); $^{13}$C{$^1$H} NMR 82.8 (s, 4C, BOC), 25.1 (s, 8C, Me); $^{11}$B{$^1$H} NMR 25.2; IR $\nu$(N−H) 3334 cm$^{-1}$. Anal. Calcd: C, 53.59; H, 9.37; N, 5.21. Found: C, 54.09; H, 9.58; N, 5.22.

**Synthesis of RHN(Bpin) (R = Ph (12), Ad (13)).** These compounds were prepared in a similar fashion using either the Et$_3$PNR or *n*-Bu$_3$PNR derivatives, and thus, only a representative preparation is detailed. HBpin (0.3 mL, 2.06 mmol) was added slowly to a 5 mL pentane solution of PhNP*n*-Bu$_3$ (0.576 g, 1.96 mmol) resulting in a bright yellow solution. After 6 h of stirring, a colorless solution remained. At −33 °C the product precipitated as a white crystalline solid in 48% yield. Preparation from Et$_3$PNPh gave **12**. Data for **12**: yield 81%; $^1$H NMR 7.09 (m, 4H, *m*-Ph, *o*-Ph), 6.77 (t, 1H, *p*-Ph, $^3J_{H-H}$ = 7 Hz), 1.07 (s, 12H, Me); $^{13}$C{$^1$H} NMR 144.3 (s, *ipso*-Ph), 129.6 (s, *m*-Ph), 120.8 (s, *o*-Ph), 118.4 (s, *p*-Ph), 83.0 (s, BOC), 25.0 (s, Me); $^{11}$B{$^1$H} NMR 24.1; IR $\nu$(N−H) 3357 cm$^{-1}$. Anal. Calcd: C, 65.79; H, 8.28; N, 6.39. Found: C, 65.56; H, 8.21; N, 6.62. Data for **13**: yield 83%; $^1$H NMR 2.37 (s, 1H, NH), 1.93 (s, 3H, Ad-CH), 1.81 (s, 6H, Ad-$CH_2$), 1.52 (m, 6H, Ad-$CH_2$), 1.14 (s, 12H, Me); $^{13}$C{$^1$H} NMR (partial) 46.0 (Ad-$CH_2$), 37.0 (Ad-$CH_2$), 30.7 (Ad-CH), 25.1 (CMe); $^{11}$B{$^1$H} NMR 24.1. Anal. Calcd: H, 10.18; C, 69.33; N, 5.05. Found: H, 9.59; C, 69.77; N, 4.66.

**Kinetic Experiments.** Using a 1.5 M stock solution of Et$_3$PNSiMe$_3$ in toluene, aliquots (0.05, 0.1, 0.2, 0.4, or 0.6 mL) were added to each of five 2 mL volumetric flasks containing HBpin (1 mL) and the integration reference PPh$_3$ (0.25 mL, 0.3 M in toluene). Similarly, aliquots of a 0.69 M stock solution of HBpin in toluene (0.57, 0.45, 0.34, or 0.227 mL) were added to Et$_3$PNSiMe$_3$ (0.5 g) and the Ph$_3$P reference solution. Aliquots of each solution were placed in a resealable NMR tube. The NMR tubes were heated in an oil bath maintained at 55 °C for the duration of the experiment. All of the above reactions were monitored using $^{31}$P{$^1$H} NMR spectroscopy. Each data set was collected at varying time intervals over a period of 7 days. Each spectrum was recorded with 32 consecutive 30° pulses and 1 s delay time. This delay time was shown to be adequate on the basis of the experiments conducted with varying delay times between pulses (1, 5, 10, 25, and 60 s) and known concentrations of reactants and products.

**Computational Studies.** Density functional theory calculations were carried out using the Gaussian 98[30] suite of programs. The B3 exchange functional,[31,32] as implemented in GAUSSIAN 98,[33] was used in combination with the correlation functional of Lee, Yang, and Parr (LYP).[34] Optimized geometries[35] were obtained using the B3-LYP functional in conjunction with the 6-31G(d) basis set. Harmonic vibrational frequencies and zero-point vibrational energy (ZPVE) corrections were also calculated at this level of theory. Relative energies were calculated by performing single point energy calculations at the B3-LYP/6-311+G(2df,p) level using the above geometries, i.e., B3-LYP/6-311+G(2df)//B3-LYP/6-31G(d,p)+ZPVE. All bond lengths are in angstroms (Å) unless otherwise specified.

**X-ray Data Collection and Reduction.** Crystals were manipulated and mounted in capillaries in a glovebox, thus maintaining a dry, O$_2$-free environment for each crystal. Diffraction experiments were performed on a Siemens SMART System CCD diffractometer. The data were collected in a hemisphere of data in 1329 frames with 10 s exposure times. The observed extinctions were consistent with the space groups in each case. The data sets were collected ($4.5° < 2\theta < 45-50.0°$). A measure of decay was obtained by recollecting the first 50 frames of each data set. The intensities of reflections within these frames showed no statistically significant change over the duration of the data collections. The data were processed using the SAINT and XPREP processing packages. An empirical absorption correction based on redundant data was applied to each data set. Subsequent solution and refinement was performed

(30) Frisch, M. J.; Trucks, G. W. S., H. B.; Scuseria, G. E.; Robb, M. A.; Cheeseman, J. R.; Zakrzewski, V. G.; Montgomery, J. A., Jr.; Stratmann, R. E.; Burant, J. C.; Dapprich, S.; Millam, J. M.; Daniels, A. D.; Kudin, K. N.; Strain, M. C.; Farkas, O.; Tomasi, J.; Barone, V.; Cossi, M.; Cammi, R.; Mennucci, B.; Pomelli, C.; Adamo, C.; Clifford, S.; Ochterski, J.; Petersson, G. A.; Ayala, P. Y.; Cui, Q.; Morokuma, K.; Malick, D. K.; Rabuck, A. D.; Raghavachari, K.; Foresman, J. B.; Cioslowski, J.; Ortiz, J. V.; Stefanov, B. B.; Liu, G.; Liashenko, A.; Piskorz, P.; Komaromi, I.; Gomperts, R.; Martin, R. L.; Fox, D. J.; Keith, T.; Al-Laham, M. A.; Peng, C. Y. N., A.; Gonzalez, C.; Challacombe, M.; Gill, P. M. W.; Johnson, B. G.; Chen, W.; Wong, M. W.; Andres, J. L.; Head-Gordon, M.; Replogle, E. S.; Pople, J. A., *Gaussian 98 and 03*; Gaussian, Inc.: Pittsburgh, PA, 1998 and 2003.
(31) Becke, A. D. *J. Chem. Phys.* **1993**, *98*, 5648−52.
(32) Becke, A. D. *J. Chem. Phys.* **1993**, *98*, 1372.
(33) Stephens, P. J.; Devlin, F. J.; Chabalowski, C. F.; Frisch, M. J. *J. Phys. Chem.* **1994**, *98*, 11623.
(34) Lee, C.; Yang, W.; Parr, R. G. *Phys. Rev. B* **1988**, *37*, 785.
(35) Optimized geometries and relative energies were also obtained at the MP2/6-31G(d,p) level of theory. The structures and relative energetics obtained are similar to those obtained at the B3-LYP/6-31G(d,p) level.

**Table 1.** Crystallographic Data[a]

| | **1** | **2** | **3**·$CH_2Cl_2$ | **4** | **5** | **6** | **11** | **12** |
|---|---|---|---|---|---|---|---|---|
| formula | $H_{19}C_{12}BNO_2P$ | $H_{31}C_{18}BNO_2P$ | $H_{19}C_{24}BNO_2P$·$CH_2C_{l2}$ | $H_{25}C_{15}BNO_2P$ | $H_{31}C_{18}BNO_2P$ | $H_{31}C_{18}BNO_2P$ | $H_{25}B_2C_{12}NO_4$ | $H_{18}BC_{12}NO_2$ |
| fw | 251.07 | 335.23 | 494.16 | 293.14 | 335.23 | 335.23 | 268.95 | 219.09 |
| *a* (Å) | 10.189(2) | 10.007(5) | 13.7714(6) | 12.298(2) | 8.593(2) | 14.167(7) | 12.400(6) | 9.928(6) |
| *b* (Å) | 11.550(3) | 10.283(5) | 9.5732(5) | 9.093(1) | 16.421(3) | 10.073(5) | 10.446(5) | 11.970(7) |
| *c* (Å) | 11. 881(3) | 10.035(5) | 17.6408(9) | 15.410(2) | 13.797(3) | 15.201(8) | 12.336(6) | 12.500(7) |
| α (deg) | 90 | 65.115(8) | 90 | 90 | 90 | 90 | 90 | 111.68(1) |
| *β* (deg) | 102.538(5) | 84.46(1) | 96.568(1) | 101.719(3) | 103.341(5) | 113.254(9) | 90.24(1) | 92.85(1) |
| *γ* (deg) | 90 | 61.646(7) | 90 | 90 | 90 | 90 | 90 | 112.435(9) |
| cryst syst | monoclinic | triclinic | monoclinic | monoclinic | monoclinic | monoclinic | monoclinic | triclinic |
| space group | $P2_1/c$ | $P\bar{1}$ | $P2_1/n$ | $P2_1/n$ | $P2_1/n$ | $P2_1/n$ | $P2_1/c$ | $P\bar{1}$ |
| *V* (Å$^3$) | 1364.9(5) | 980.3(8) | 2310.4(2) | 1687.1(3) | 1894.3(6) | 1993(2) | 1597(1) | 1244(1) |
| *d*(calc) (g cm$^{-1}$) | 1.217 | 1.136 | 1.380 | 1.154 | 1.175 | 1.117 | 1.118 | 1.170 |
| Z | 4 | 2 | 6 | 4 | 4 | 4 | 2 | 2 |
| abs coeff, *μ* (cm$^{-1}$) | 0.191 | 0.148 | 0.374 | 0.163 | 0.154 | 0.146 | 0.079 | 0.077 |
| data collcd | 6502 | 4227 | 11201 | 8148 | 9150 | 8264 | 6628 | 5307 |
| data $F_o^2 > 3\sigma(F_o^2)$ | 1962 | 2810 | 3335 | 2423 | 2722 | 2830 | 2287 | 3508 |
| variables | 154 | 208 | 289 | 181 | 208 | 208 | 175 | 290 |
| $R^b$ | 0.0727 | 0.0477 | 0.0618 | 0.0559 | 0.0832 | 0.0366 | 0.0552 | 0.0687 |
| $R_w^c$ | 0.012 02 | 0.0662 | 0.0943 | 0.1123 | 0.1601 | 0.0534 | 0.0863 | 0.1695 |
| GOF | 1 .052 | 1.000 | 1.033 | 1.012 | 1.024 | 0.884 | 1.026 | 1.003 |

[a] These data were collected at 20 °C with Mo Kα radiation ($\lambda$ = 0.710 69 Å). [b] $R = \Sigma(F_o - F_c)/\sigma(F_o)$. [c] $R_w = \{\Sigma[w(F_o^2 - F_c^2)^2]/\Sigma[\sigma(F_o)^2]\}^{1/2}$.

using the SHELXTL solution package. Crystallographic data are listed in Table 1.

**Structure Solution and Refinement.** Non-hydrogen atomic scattering factors were taken from literature tabulations.[36] The heavy atom positions were determined using direct methods employing the SHELXTL direct methods routine. The remaining non-hydrogen atoms were located from successive difference Fourier map calculations. The refinements were carried out by using full-matrix least- squares techniques on *F*. In the final cycles of each refinement, all non-hydrogen atoms were assigned anisotropic temperature factors in the absence of disorder or insufficient data. In the latter cases atoms were treated isotropically. C−H atom positions were calculated and allowed to ride on the carbon to which they are bonded. H-atom temperature factors were fixed at 1.10 times the isotropic temperature factor of the C-atom to which they are bonded. The H-atom contributions were calculated but not refined. The locations of the largest peaks in the final difference Fourier map calculation as well as the magnitude of the residual electron densities in each case were of no chemical significance. Additional details are provided in the Supporting Information.

## Results and Discussion

The catecholboryl−phosphinimide complexes of the general formula ($\mu$-($R_3$PN)Bcat))$_x$ (R = Et **(1)**, *n*-Bu **(2)**, Ph **(3)**, *i*-Pr **4**, *t*-Bu **(6)**, $R_3$ = *n*-Bu *t*-$Bu_2$ **(5)**) were synthesized via the straightforward metathetical reaction of the corresponding $R_3PNSiMe_3$ and ClBcat in toluene at room temperature (Scheme 1). The $^{31}P\{^1H\}$ chemical shifts of compounds **1**−**6** are downfield shifted relative to the starting material $R_3PNSiMe_3$, consistent with the deshielding of the phosphorus center by the electron-withdrawing boron atom. All of the resulting derivatives were characterized by $^1H$, $^{31}P\{^1H\}$, $^{11}B\{^1H\}$, and $^{13}C\{^1H\}$ NMR spectroscopy, elemental analysis, and X-ray crystallography. These data were consistent with the empirical formulation although the nature of the oligomerization could not be unambiguously determined.

**Scheme 1**

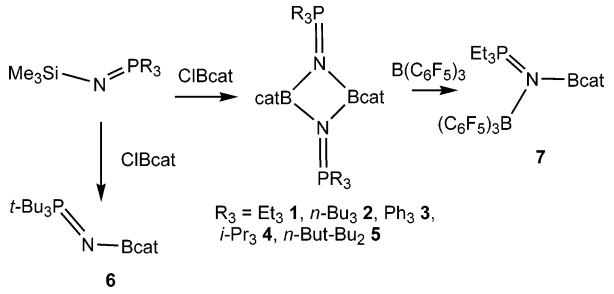


Single-crystal X-ray diffraction studies revealed that complexes **1**−**5** are dimeric in the solid state and thus formulated as ($\mu$-($R_3$PN)Bcat)$_2$. These molecules have similar structures, and representative ORTEP drawings of **1** and **3** are presented in Figures 1 and 2. In these compounds, the phosphinimide nitrogen atoms bridge the two B centers giving a planar four-membered $B_2N_2$ core with B−N−B′ and N−B−N′ angles that are all very close to 90°. The resulting coordination sphere about B is thus composed of two N-atoms and the two O-atoms of the catecholate ligand yielding a pseudotetrahedral geometry. The N−B bond distances in **1**−**5** range from 1.529(5) to 1.573(6) Å, which are slightly longer than those observed for (($Br_2B$($\mu$-

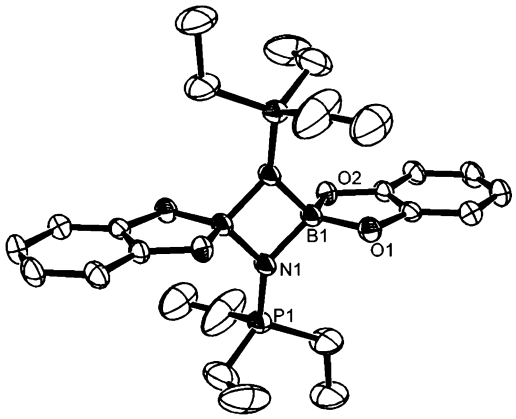


**Figure 1.** ORTEP drawing of **1** with 30% thermal ellipsoids. Hydrogen atoms are omitted.

(36) Cromer, D. T.; Waber, J. T. *Int. Tables X-ray Crystallogr.* **1974**, *4*, 71−147.

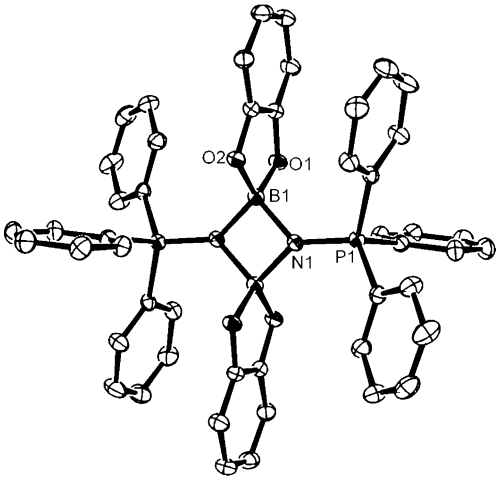


**Figure 2.** ORTEP drawing of **3** with 30% thermal ellipsoids. Hydrogen atoms are omitted.

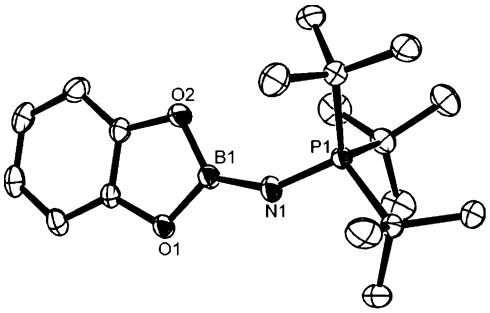


**Figure 3.** ORTEP drawing of **6** with 30% thermal ellipsoids. Hydrogen atoms are omitted.

$NPMe_3))_2$ (1.504(4) Å), $(Cl_2B(\mu\text{-}NPPh_3))_2$ (1.527(2) Å), and $(Cl_2B(\mu\text{-}NPEt_3))_2$ (1.510(2) Å).[37,38] The longer bond lengths in **1**−**5** are attributed to the presence of the electron-donating catecholate fragment. The P−N distances in **1**−**5** vary from 1.563(4) to 1.607(2) Å. The P−N−B angles range from 127.9(2) to 135.4(3)° and are generally correlated to the steric bulk of substituents on P.

The X-ray crystallographic data for **6** revealed a monomeric structure (Figure 3). The P−N distance of 1.563(2) Å is longer than those seen in **2**−**5** and the average P−N bond lengths of the monomeric borylphosphinimide complexes: $B(NPPh_3)_3$ (1.549(5) Å) and $HB(NPt\text{-}Bu_3)_2$ (1.531(5) Å).[20,21] The B−N distance of 1.369(3) Å is much shorter than those observed for **1**−**5** and those seen for $B(NPPh_3)_3$ (1.45(1) Å) and $HB(NPt\text{-}Bu_3)_2$ (1.41(5) Å). The geometry about B is approximately trigonal-planar with N−B−O angles of 123.6(2) and 128.8(2)° and a P−N−B angle of 145.6(2)°. This latter, relatively large angle is consistent with N to B $\pi$-donation. The monomeric nature of **6** is attributed to the steric bulk of the *tert*-butyl groups. The steric demands of the $Pt\text{-}Bu_3$ fragment have been recognized since Tolman developed the notion of cone angles.[39]

The dimeric nature of **1**−**5** in solution was probed. The $^{11}B\{^1H\}$ NMR shift for compounds **1**−**4** ranges between 6.0 and 8.4 ppm, typical of four-coordinate B and thus consistent with a dimeric structure in solution. In the case of **6** the $^{11}B\{^1H\}$ NMR shift is 24.2 ppm typical of three-coordinate B, that is, a monomeric compound[40−44] consistent with the solid-state structure. Compound **5** which is dimeric in the solid state exhibits a $^{11}B\{^1H\}$ NMR shift at 24.4 ppm. This implies a monomer−dimer equilibrium in solution that favor a monomer in solution. Such an equilibrium is also indicated by $^{31}P\{^1H\}$ NMR spectroscopy on a mixture of **1** and **4**. While both compounds gives rise to a single resonance in the $^{31}P\{^1H\}$ NMR spectrum, the mixture shows these signals as well as two additional sets of doublets. The latter resonances were was attributed to the dissymmetric dimer $(\mu\text{-}Et_3PN)(Bcat)_2(\mu\text{-}i\text{-}Pr_3PN)$ (Figure 4). The P−P coupling between the P centers was observed to be 21 Hz. This exchange suggests that some small degree of dissociation of the dimers **1** and **4** occurs in solution allowing recombination to give the observed statistical mixture of all possible dimers. Similar exchange experiments were also conducted using **2** and **6**. This resulted only in the observation of the resonances attributable to **2** and **6**. This supports the view that compound **6** retains its monomeric nature both in solution and in the solid state. This is likely due to the steric crowding about the N atom which precludes further association.

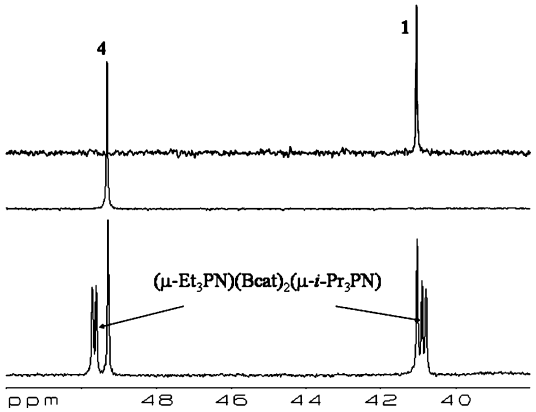


**Figure 4.** $^{31}P\{^1H\}$ NMR spectra of **1**, **4**, and mixture of **1**, **4**, and $(\mu\text{-}Et_3PN)(Bcat)_2(\mu\text{-}i\text{-}Pr_3PN)$.

In a similar vein, **1** reacts with with 2 equiv of $B(C_6F_5)_3$ to give the quantitative formation of $(\mu\text{-}Et_3PN)Bcat(B(C_6F_5)_3)$ **7** (Scheme 1). Spectroscopic data support this formulation. In particular, the $^{31}P\{^1H\}$ NMR resonance shifts downfield to 68.0 ppm, consistent with coordination of the electron-deficient borane to the phosphinimide-N atom. In contrast and consistent with the above exchange studies, addition of

(37) Moehlen, M.; Harms, K.; Dehnicke, K.; Magull, J.; Goesmann, H.; Fenske, D. *Z. Anorg. Allg. Chem.* **1996**, *622*, 1692−1700.
(38) Moehlen, M.; Neumuller, B.; Faza, N.; Muller, C.; Massa, W.; Dehnicke, K. *Z. Anorg. Allg. Chem.* **1997**, *623*, 1567−1576.
(39) Tolman, C. A. *Chem. Rev.* **1977**, *77*, 313−348.
(40) Clegg, W.; Dai, C.; Lawlor, F. J.; Marder, T. B.; Nguyen, P.; Norman, N. C.; Pickett, N. L.; Power, W. P.; Scott, A. J. *Dalton Trans.* **1997**, 839−846.
(41) Coapes, R. B.; Souza, F. E. S.; Fox, M. A.; Batsanov, A. S.; Goeta, A. E.; Yufit, D. S.; Leech, M. A.; Howard, J. A. K.; Scott, A. J.; Clegg, W.; Marder, T. B. *Dalton Trans.* **2001**, 1201−1209.
(42) Marder, T. B.; Smith, P. S.; Howard, J. A. K.; Fox, M. A.; Mason, S. A. *J. Organomet. Chem.* **2003**, *680*, 165−172.
(43) Nguyen, P.; Dai, C.; Taylor, N. J.; Power, W. P.; Marder, T. B.; Pickett, N. L.; Norman, N. C. *Inorg. Chem.* **1999**, *34*, 4290−4291.
(44) Wescott, S. A.; Blom, H. P.; Marder, T. B.; Baker, R. T.; Calabrese, J. C. *Inorg. Chem.* **1993**, *32*, 2175−2182.

**Scheme 2**

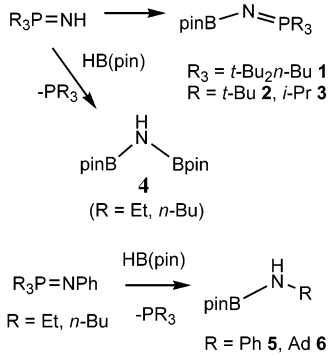


the Lewis acidic $B(C_6F_5)_3$ to the monomeric complex **6** results in no change in the NMR spectra, again reflecting the steric congestion about the nitrogen atom in **6**.

Reactions of R(*t*-Bu)$_2$PNH (R = *n*-Bu, *t*-Bu) with HBpin led to vigorous evolution of $H_2$ and the formation of the compounds of empirical formulas R(*t*-Bu)$_2$PNBpin (R = *n*-Bu (**8**), *t*-Bu (**9**)) (Scheme 2). These species were isolated as colorless oils after a few minutes reaction time in toluene or pentane solution, in yields of 61 and 94%, respectively. Similarly, reaction of 1 equiv of *i*-Pr$_3$PNH with 1 equiv of HBpin in toluene at box temperature produced the borylphosphinimide of empirical formula *i*-Pr$_3$PNBpin (**10**) as the major product in 87% yield. The $^1$H, $^{31}$P{$^1$H}, $^{13}$C{$^1$H}, and $^{11}$B{$^1$H} NMR spectra were consistent with the above formulations. The $^{11}$B NMR shifts for **8**−**10** all range from 22.6 to 23.9 ppm typical of three-coordinate B centers implying that all of these species are monomeric in solution.[40−44] This is not surprising given the lower Lewis acidity of Bpin derivatives in comparison to Bcat analogues. Interestingly, solutions of both **8** and **10** gave rise to downfield $^{31}$P resonances upon addition of $B(C_6F_5)_3$ presumably as a result of the generation of $(R_3PNBpin)B(C_6F_5)_3$, whereas the analogous addition to a solution of **9** results in no apparent reaction. The absence of reaction in the latter case is attributable to steric demands of the phosphinimide ligand.

Reaction of smaller phosphinimines $R_3PNH$ (R = Et or *n*-Bu) with HBpin also resulted in the liberation of $H_2$. However, monitoring these reactions by $^{31}$P{$^1$H} NMR spectroscopy revealed the generation of the corresponding free phosphines. Subsequently, the boron-containing product HN(Bpin)$_2$ (**11**) was isolated as a white solid. $^1$H NMR data revealed only the presence of the pinacolate protons, and IR spectral data revealed an absorption at 3334 cm$^{-1}$ consistent with the presence of an N−H fragment. X-ray-quality crystals of **11** were grown from pentane, and the X-ray data confirmed the formulation as the diborylamine (Figure 5). The B−N bond distances in **11** average 1.419(6) Å, which is typical for B−N bond distances in diborylamines.[45−48]

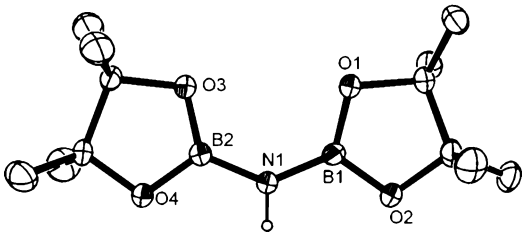


**Figure 5.** ORTEP drawing of **11** with 30% thermal ellipsoids. Hydrogen atoms are omitted. Selected distances (Å) and angles (deg): B(1)−O(1) 1.370(4), B(1)−O(2) 1.390(4), B(1)−N(1) 1.418(4), B(2)−O(3) 1.348(4), B(2)−O(4) 1.384(4), B(2)−N(1) 1.421(4); O(1)−B(1)−O(2) 112.5(3), O(1)−B(1)−N(1) 126.7(3), O(2)−B(1)−N(1) 120.8(3), O(3)−B(2)−O(4) 112.7(2), O(3)−B(2)−N(1) 126.1(3), O(4)−B(2)−N(1) 121.3(3), B(1)−N(1)−B(2) 132.9(3).

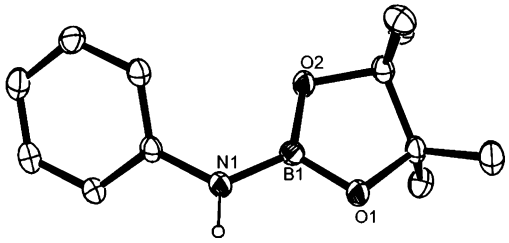


**Figure 6.** ORTEP drawing of **12** with 30% thermal ellipsoids. Hydrogen atoms are omitted. Selected distances (Å) and angles (deg): N(1)−B(1) 1.406(4), N(1)−C(7) 1.411(3), O(1)−B(1) 1.378(3), O(2)−B(1) 1.376(3); B(1)−N(1)−C(7) 126.8(2), O(2)−B(1)−O(1) 113.5(2), O(2)−B(1)−N(1) 124.3(2), O(1)−B(1)−N(1) 122.1(2).

Location and refinement of the proton on nitrogen revealed that the geometry at N is planar, with a B−N−B angle of 132.9(3)°. This angle is similar to the corresponding angle of 135.4(2)° observed for HN(BPh$_2$)$_2$.[47]

In the related reactions of $R_3PNPh$ or $R_3PNAd$ (R = Et and *n*-Bu) with HBpin, $^{31}$P{$^1$H} NMR spectroscopy revealed the liberation of free phosphine, consistent with reduction of the phosphinimine precursor. Subsequent workup afforded the white crystalline solid PhHN(Bpin) (**12**) and AdHN(Bpin) (**13**) in yields of 81% and 83%, respectively. A crystallographic study of **12** revealed a similar geometry with a B−N bond length of 1.406(4) Å and an C−N−B angle of 126.8(2)° (Figure 6).

The formation of **11** from the reaction of phosphinimine and HBpin was rapid; however, the species $Et_3PNSiMe_3$ was shown to react with HBpin at a much slower rate, such that the kinetics could be monitored. Reactions of excess HBpin with varying concentrations of $Et_3PNSiMe_3$ were performed and monitored as a function of time at 55 °C. $Ph_3P$ was used as an internal integration standard. The formation of $Et_3P$ and the consumption of $Et_3PNSiMe_3$ revealed that the rate-determining step exhibits a first-order dependence on the concentration of $Et_3PNSiMe_3$ (Figure 7a). Analogous experiments using varying concentrations of HBpin and excess $Et_3PNSiMe_3$ revealed that the reaction is first order in HBpin (Figure 7b). The overall rate constant at 55 °C, *k*, was determined to be 1.3(7) × 10$^{-4}$ s$^{-1}$. On the basis of these data, a mechanism involving a 1:1 donor−acceptor interaction of the phosphinimine and borane is proposed to prompt

(45) Al-Juaid, S. S.; Eaborn, C.; Hitchcock, P. B.; Kundu, K. K.; Molla, M. E.; Smith, J. D. *J. Organomet. Chem.* **1990**, *385*, 13−21.
(46) Bartlett, R. A.; Chen, H.; Dias, H. V. R.; Olmstead, M. M.; Power, P. P. *J. Am. Chem. Soc.* **1988**, *110*, 446−9.
(47) Maennig, D.; Noeth, H.; Prigge, H.; Rotsch, A. R.; Gopinathan, S.; Wilson, J. W. *J. Organomet. Chem.* **1986**, *310*, 1−20.
(48) Paciorek, K. J. L.; Kratzer, R. H.; Kimble, P. F.; Nakahara, J. H.; Wynne, K. J.; Day, C. S. *Inorg. Chem.* **1988**, *27*, 2432−6.

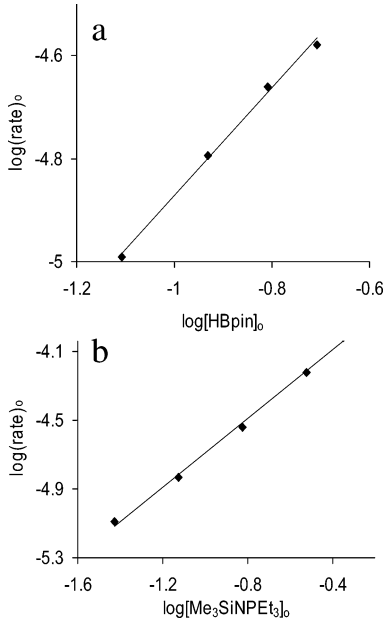


**Figure 7.** (a) Plot of log (rate)$_o$ versus log[$Et_3PNSiMe_3$]$_o$. (b) Plot of log(rate)$_o$ versus log[HBpin]$_o$.

**Scheme 3**

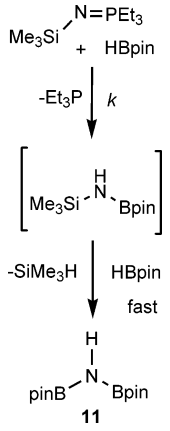


the rate-determining reduction of the phosphinimine to phosphine with the formation of the borylamine. This view is supported by the isolation of **12** and **13**. A rapid reaction generating **11** follows (Scheme 3). Attempts to obtain thermodynamic data for this reaction were thwarted by the thermal decomposition of the HBpin above 55 °C and the extremely slow reaction of $Et_3PNSiMe_3$ and HBpin at temperatures below 55 °C.

The formation of **8**−**11** clearly demonstrates two reaction pathways are accessible in the parent reaction of $R_3PNH$ and HBpin. Computations at the B3LYP/6-311G(2df,p) level on the two reaction pathways for *t*-$Bu_3PNH$ or $H_3PNH$ with $HB(OCH_2)_2$ indicate that both $H_2$ elimination and phosphinimine reduction are thermodynamically favorable. However, for the model reactions involving *t*-$Bu_3PNH$, the activation barrier to $H_2$ elimination is 11.8 kcal/mol (Figure 8) lower than that of the reaction pathway involving phosphinimine reduction. In contrast, for the reactions modeled with $H_3PNH$ the differences in the activation barriers are much smaller with phosphinimine reduction being favored by 2.3 kcal/mol (Figure 9). While this small difference suggests that

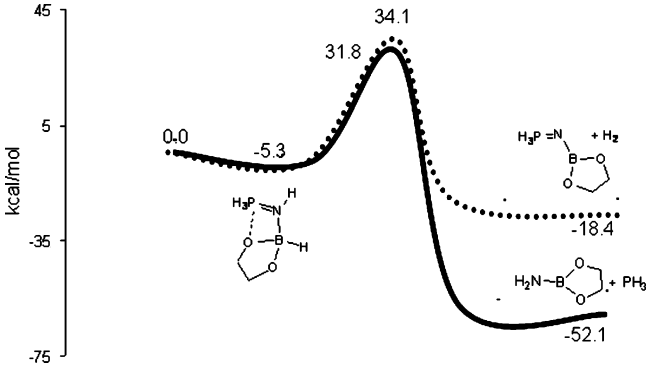


**Figure 8.** Schematic gas-phase potential energy surface for the reactions of $H_3PNH$ with $HB(OCH_2)_2$.

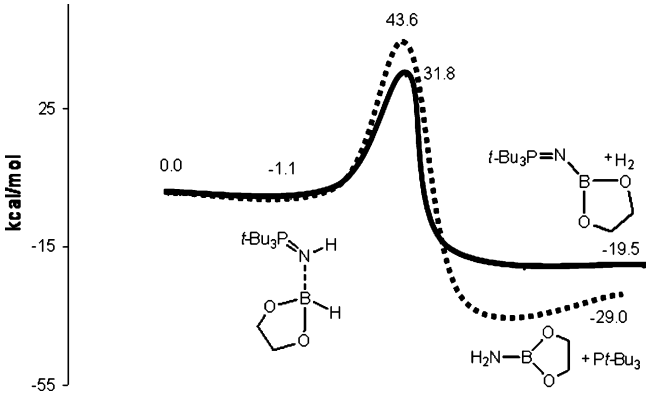


**Figure 9.** Schematic gas-phase potential energy surface for the reaction of *t*-$Bu_3PNH$ with $HB(OCH_2)_2$.

both pathways should be accessible for sterically less demanding phosphinimines at room temperature, this is not observed experimentally. This observation suggests that the differences in the activation energies are underestimated. This could reflect a limitation of these gas-phase computations and the need to consider solvation and temperature effects. Nonetheless, the computational model data predict a crossover in preference from one pathway to the other with changing the steric demands, an observation that is confirmed experimentally.

The optimized geometries of the phosphinimine−borane adducts $(H_3PNH)HBO_2C_2H_4$, $(H_3PNH)HBpin$, (*t*-$Bu_3PNH$)-$HBO_2C_2H_4$, and (*t*-$Bu_3PNH$)HBpin shed some light on this issue on the differing pathways. These computations predict that the adducts are pseudotetrahedral at B and trigonal planar at N with B−N distances of 1.56, 1.60, 1.60, and 1.61 Å, respectively (Figure 10). Interestingly, the differences among these models are the orientations of substituents about the B−N bonds. In the case of $(H_3PNH)HBO_2C_2H_4$ and $(H_3PNH)HBpin$, the P-atom is oriented in close proximity to one of the O-atoms of the diolate on boron (P···O: 2.13 and 2.25 Å) (Figure 10a). This proximity is evident in the Newman projection (Figure 10b) down the B−N bond which shows the almost eclipsed nature of the P on N and O on B. This geometry, which provides a pseudo-OBNP four-membered ring, is reminiscent of the proposed phosphetidine intermediate for phosphinimine metathesis.[9] In the optimized structures of (*t*-$Bu_3PNH$)$HBO_2C_2H_4$ and (*t*-$Bu_3PNH$)HBpin, these P···O distances are increased to 3.47 and 3.53 Å, re-

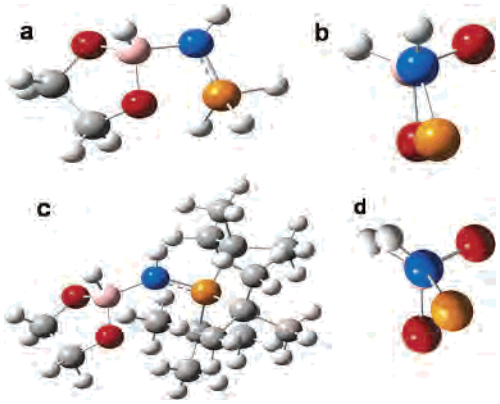


**Figure 10.** Optimized structures for (a) $(H_3PNH)HBO_2C_2H_4$ and (b) $(t\text{-}Bu_3PNH)HBO_2C_2H_4$. The corresponding Newman projections down the B−N vector are shown in (c) and (d), respectively. Color scheme: O, red; B, pink; N, blue; P, orange.

spectively (Figure 10c,d). Previous computational studies[14−16] have noted the polarized nature of the P−N bond in phosphinimines. Thus, the closer approach of P and O with decreasing steric demands of the substituents on P in the present systems suggests that the lowest energy orientation about the B−N bond is determined by electrostatic attraction between P($\delta$+) and the boron-bound oxygen atoms ($\delta$−).

In the optimized geometry of $(H_3PNH)HBO_2C_2H_4$ and $(H_3PNH)HBpin$, the dihedral angles between the BH and NH groups are 63.5 and 38.3°, respectively. This geometry results in a BH···HN separations of 2.90 and 2.70 Å. As the steric bulk of the substituents is increased in the models, $(t\text{-}Bu_3PNH)HBO_2C_2H_4$ and $(t\text{-}Bu_3PNH)HBpin$, the corresponding H−N−B−H dihedral angles decrease to 4.43 and 10.86°, respectively, while the H···H separations decrease to 2.20 and 2.13 Å, respectively. These data suggest that sterically demanding substituents prompt closer proximity of B- and N-bound H-atoms and thus favor $H_2$ elimination and formation of *N*-borylphosphinimines. In contrast, for phosphinimines with small substituents, the preferred orientation in the intermediate adducts is dictated by the electrostatic P···O attraction. The result is a staggered position of the B- and N-bound H-atoms and an increased separation. In this orientation, hydride transfer from B to N is favored, resulting in the reduction of the phosphinimine. Such hydride transfer for reactions of $HNPR_3$ affords the transient $H_2NBpin$ which reacts rapidly with a second 1 equiv of HBpin to give **11** while the analogous reaction for $RNPEt_3$ (R = Ph, Ad) provides **12** and **13** directly.

## Summary

Catecholborane−phosphinimide derivatives are easily formed via reactions of chlorocatecholborane and silylphosphinimines. Steric factors determine whether the products are monomers or dimers. Reactions of phosphinimines and pinacolborane proceed via two pathways. In the case of sterically demanding phosphinimines, pinacolborane−phosphinimide derivatives are obtained. In the case of phosphinimines with less demanding substituents on P, reduction to free phosphine and the formation of borylamines occurs. These differing pathways can be attributed to the role of steric effects determining the orientation about the B−N bond in the intermediate phosphinimine−borane adducts. The study of the effects of steric factors on the reactivity of phosphinimines and their derivatives continues to be the subject of investigation in our group.

**Acknowledgment.** Financial support from the NSERC of Canada (D.W.S., J.W.G.) and NOVA Chemicals Corp. (D.W.S.) is gratefully acknowledged. S.H. is grateful for the award of an Ontario Graduate Scholarship. We also thank Professor Todd Marder of the University of Durham for his insightful comments.

**Supporting Information Available:** Crystallographic data in CIF format. This material is available free of charge via the Internet at http://pubs.acs.org. CIF files are available on-line from the Cambridge Crystallographic Data Centre (CCDC Nos. 235138−235140 and 263395−263399).

IC050230K